Abstract #05290 ISMRM ABSTRACT

Improved Monitoring of Injectable Biomaterial Implants in Rats Using Dixon-TurboRARE MRI at 9.4T

Primary: Analysis Methods - Segmentation and Detection 〉 **Secondary:** Preclinical Animal & in vitro MR - Small Animals 〉 **Digital Poster** · 55 min | Novel Neuro Applications · Wednesday, May 13 at 08:20 AM 〉 **Keywords:** PRECLINICAL IMAGE ANALYSIS DIXON-MRI VOLUMETRIC SEGMENTATION SUBCUTANEOUS IMPLANTS

Omar Zenteno [1,2], **Aly Elbindary**[1,2], **Constance Lesage**[1,2], **Estelle Gerossier**[1,2], **jocelyn Grosse**[1,2], **Bernard Lanz**[1,2]

[1]CIBM Center for Biomedical Imaging, Lausanne, Switzerland
[2]CIBM Pre-Clinical Imaging EPFL Metabolic Imaging Section, École polytechnique fédérale de Lausanne - EPFL, Lausanne, Switzerland

Presenting Author: *Omar Zenteno (omar.zenteno@epfl.ch)*

Impact

Volumetric assessment is critical for implant studies in rat models. Results showed that caliper measurements systematically overestimated implant size, whereas Dixon-based MRI with automated segmentation (SAM) achieved high accuracy and reproducibility, establishing a standardized preclinical imaging framework with translational value.

Synopsis

Motivation: Conventional T2-weighted MRI obscures subcutaneous implant boundaries from fat contamination and chemical shift, limiting accurate longitudinal volumetry.

Goals: Establish a reproducible Dixon-based MRI method for implant delineation and volumetric analysis in rats

Approach: Dixon-TurboRARE imaging at 9.4T generated water- and fat-only reconstructions. Caliper measurements and manual MRI segmentation were compared across all timepoints (D0–D61). Automated segmentation (SAM) was trained on early timepoints and evaluated at day 61.

Results: Caliper overestimated implant volumes, while manual segmentation matched injected quantities but required ~120 min/rat. Automated segmentation matched manual masks (Dice >0.80) in ~10 min/rat, and volumetric comparison yielded RMSE ≈10% of mean implant volume.

Introduction

Injectable biomaterials have been proposed for volume restoration following implantation [1, 2]. In preclinical studies, these materials are delivered subcutaneously in small-animal models, where longitudinal monitoring is essential to evaluate their volume. Reliable volumetric quantification, however, remains challenging. Caliper measurements, though common, capture only superficial dimensions and often misestimate true implant size. Recent work has demonstrated pipelines for automatic segmentation of implants on T2-weighted MRI [3], yet this contrast is limited by fat contamination and chemical shift artifacts that obscure boundaries. Dixon imaging, by separating water and fat signals, generates component-specific reconstructions that enhance implant conspicuity and provide a reproducible basis for reliable segmentation and volumetric analysis.

Methods:

A total of 32 subcutaneous implants (n = 32) were placed in 4 adult rats, with 8 implantation sites per animal (4 dorsal and 4 ventral). Seven different implant types were tested (A-G), including the volume-stable implant (type D), which was injected at both a dorsal and a ventral site in each animal. MRI was performed at 9.4T (Bruker BioSpec) using a respiration-triggered Dixon-TurboRARE sequence (TR = 3000 ms, TE = 20 ms), ensuring T2-weighted contrast. Images were acquired with an in-plane resolution of 0.21 × 0.21 mm and a slice thickness of 1.25 mm, covering a field of view of 70 × 70 × 60 mm (Figure 1). Water and fat images were reconstructed using the ParaVision Dixon module, and imaging was performed longitudinally at days 0, 7, 14, 21, 28, and 61. Manual segmentation was carried out slice by slice in 3D Slicer [4], from which volumetric growth curves were directly derived. MRI-derived volumes were then compared with caliper measurements obtained at each timepoint. To enable automated analysis, segmentations were exported as labelmaps to build the dataset for model training. Automated segmentation was implemented using the Segment Anything Model (SAM) [5] with a ViT-H backbone pretrained on SA-1B. Fine-tuning was conducted on Dixon water images using manual masks as ground truth, optimized with AdamW (learning rate = 1e−3) for 50 epochs on a NVIDIA RTX 3060 GPU. The dataset comprised 900 2D slices for training/validation and 236 for testing. The Dice similarity coefficient (2D) was used to quantify spatial overlap, while 3D volumes were reconstructed from slice-wise predictions to enable volumetric comparison against manual references. For volumetric analysis, the original SAM mask containing all implants was split into individual connected components (islands) based on voxel neighborhood, and 3D volumes were computed from these separated regions.

Results:

MRI-derived volumes of the volume-stable implants (type D) at day 0 closely matched the injected volume of 250 mm³ (mean = 242.1 ± 68.6 mm³), confirming the accuracy of Dixon-based manual segmentation. Across timepoints, type D implants remained stable (mean = 241.4 ± 62.2 mm³), with no significant volumetric changes. To allow comparison across implant types, subsequent measurements were normalized to baseline (D0 = 1). Figure 2 shows swelling ratios derived from caliper and MRI measurements. Caliper curves exhibited higher variability and progressive divergence, whereas MRI-based ratios remained consistent across animals and implant types, reflecting improved reproducibility. Bland–Altman analysis (Figure 3) confirmed systematic caliper overestimation relative to MRI, with poor agreement at days 7 and 61 and smaller bias (+20–60%) at intermediate timepoints. Manual segmentation, while accurate, required ~120 min per rat. Automated segmentation achieved strong agreement with manual references, reducing processing time to ~10 min per rat. At day 61, regression analysis demonstrated high concordance between SAM- and manually-derived implant volumes (R^2 = 0.95, RMSE = 33.6 mm³, ~10% of mean implant volume), as shown in Figure 4, which illustrates implant overlays highlighting close boundary alignment with slight peripheral underestimation. Figure 5 complements this with a 3D visualization of Dixon water-only reconstructions and SAM overlays, confirming accurate detection and spatial correspondence of implants with the underlying anatomy.

Discussion

This study demonstrates that Dixon-based MRI enables robust longitudinal monitoring of subcutaneous implants in a rat model. Validation with volume-stable implants confirmed accurate volumetric quantification, while caliper overestimation highlighted limitations of surface-based measurements. Automated segmentation improved scalability by reducing operator dependency and analysis time. Although only water reconstructions were used, fat

reconstructions may provide complementary information. Future work will explore multimodal segmentation strategies combining water and fat images to improve boundary delineation and peri-implant tissue characterization.

Conclusion:

Dixon-based MRI with automated segmentation offers a reproducible, scalable method for quantitative monitoring of subcutaneous implants, addressing limitations of conventional measurements and providing a translational framework for standardized evaluation in preclinical and clinical settings.

Acknowledgements

Animal experiments and imaging were performed thanks to InnoSuisse grant 113.704 IP-LS. EG, JG and BL were supported by the CIBM Center for Biomedical Imaging, a Swiss research center of excellence founded and supported by Lausanne University Hospital (CHUV), University of Lausanne (UNIL), Ecole Polytechnique Fédérale de Lausanne (EPFL), University of Geneva (UNIGE) and Geneva University Hospitals (HUG).

References

1. doi:10.1002/adhm.201400250
2. doi:10.1007/s13770-021-00420-6
3. doi:10.3389/frsip.2023.1155618
4. doi:10.1016/j.mri.2012.05.001
5. doi:10.1109/ICCV51070.2023.00371

Figures and Tables

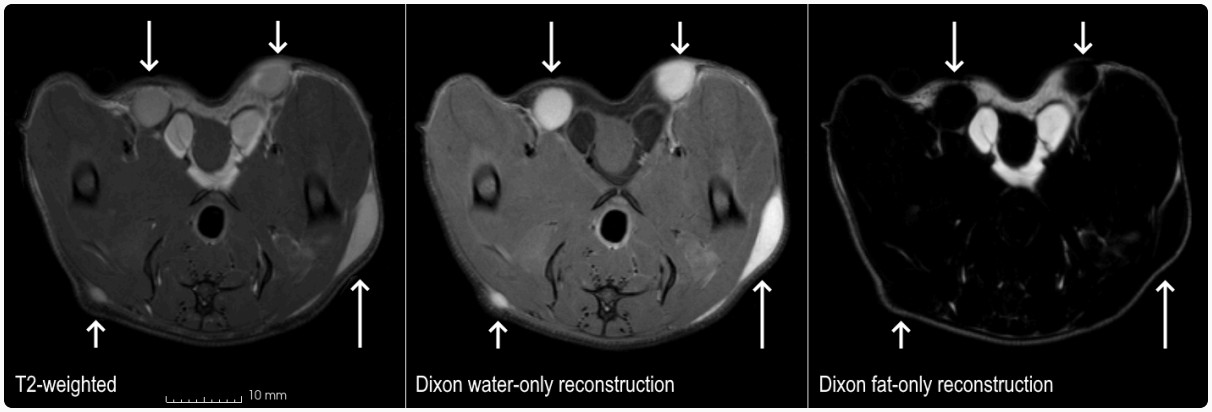

Scan for high-resolution version

Figure 1: *Representative Dixon-TurboRARE images acquired at TR = 3000 ms and TE = 20 ms. The water-only reconstruction (center) provides superior implant-to-tissue contrast (white arrows) and was selected as the primary channel for volumetric analysis. The corresponding conventional T2-weighted image (left) shows blurred implant boundaries due to chemical shift and fat signal contamination, while the fat-only image (right) highlights surrounding adipose tissue.*

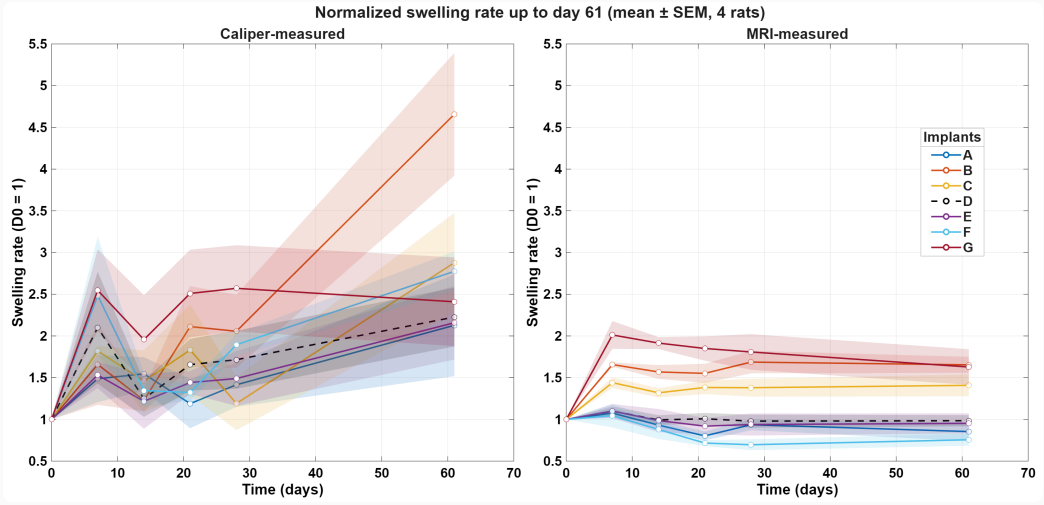

Scan for high-resolution version

Figure 2: *Normalized (D0 = 1) longitudinal swelling measurements derived from caliper and MRI for the seven implant types (A–G), shown as mean ±SEM across four rats (n = 4). The dashed black line corresponds to implant type D, expected to remain volume-stable and thereby validating the accuracy of manual MRI segmentation. Caliper-derived ratios show higher variability and overestimation, whereas MRI-derived ratios remain consistent.*

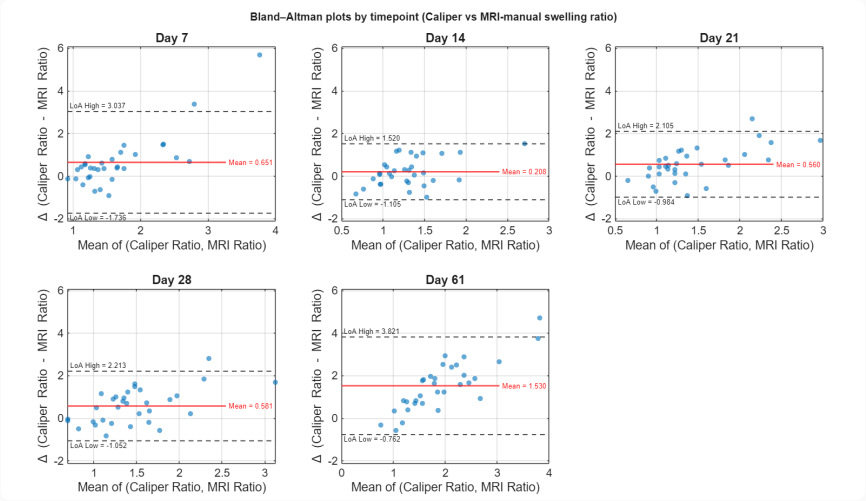

Scan for high-resolution version

Figure 3: *Bland–Altman analysis of Caliper- vs MRI-ratio for implant growth at days 7–61. Ratios are normalized as in Figure 2 (D0 = 1). Caliper consistently overestimates implant size relative to MRI, with poor agreement at day 7 and day 61, and smaller bias (+20–60%) at intermediate timepoints. Overall, MRI provides more reliable volumetric assessment across all timepoints.*

Animated Figure 4

This figure contains animation/video content. To view the animation, scan the QR code with your mobile device or visit the online version of this abstract.

Figure 4: *Left: Scatter plot of implant volumes manually segmented vs SAM (n = 31, including one case where two adjacent implants fused during expansion). Regression analysis showed strong agreement ($R^2 = 0.95$, slope = 0.81). The RMSE was 33.6 mm^3, corresponding to ~10% of the mean manual implant volume (~340 mm^3). Right: Representative 3D rendering illustrating overlap between SAM (red) and manual (white) segmentations. Areas of concordance appear pink, showing that SAM closely follows implant boundaries*

Animated Figure 5

This figure contains animation/video content. To view the animation, scan the QR code with your mobile device or visit the online version of this abstract.

Figure 5: *Video illustration of subcutaneous implant visualization at day 61. Left: 3D rendering of Dixon water-only reconstruction, showing implants at the skin surface. Right: the same volume with SAM-derived segmentation (red) overlaid, highlighting automated detection and spatial correspondence with the underlying anatomy.*